

Binding of Procollagen C-Proteinase Enhancer-1 (PCPE-1) to Heparin/Heparan Sulfate

PROPERTIES AND ROLE IN PCPE-1 INTERACTION WITH CELLS*

Received for publication, May 6, 2010, and in revised form, July 29, 2010. Published, JBC Papers in Press, August 21, 2010, DOI 10.1074/jbc.M110.141366

Tali Weiss[‡], Sylvie Ricard-Blum[§], Laura Moschovich[‡], Eitan Wineman[‡], Shlomit Mesilaty[‡], and Efrat Kessler^{‡1}

From the [‡]Maurice and Gabriela Goldschleger Eye Research Institute, Tel-Aviv University Sackler Faculty of Medicine, Sheba Medical Center, Tel Hashomer 52621, Israel and the [§]Institut de Biologie et Chimie des Protéines, UMR 5086 CNRS-Université Lyon 1, 69367 Lyon Cedex 7, France

Procollagen C-proteinase enhancer-1 (PCPE-1) is an extracellular matrix (ECM) glycoprotein that can stimulate procollagen processing by procollagen C-proteinases (PCPs) such as bone morphogenetic protein-1 (BMP-1). The PCPs can process additional extracellular protein precursors and play fundamental roles in developmental processes and assembly of the ECM. The stimulatory activity of PCPE-1 is restricted to the processing of fibrillar procollagens, suggesting PCPE-1 is a specific regulator of collagen deposition. PCPE-1 consists of two CUB domains that bind to the procollagen C-propeptides and are required for PCP enhancing activity, and one NTR domain that binds heparin. To understand the biological role of the NTR domain, we performed surface plasmon resonance (SPR) binding assays, cell attachment assays as well as immunofluorescence and activity assays, all indicating that the NTR domain can mediate PCPE-1 binding to cell surface heparan sulfate proteoglycans (HSPGs). The SPR data revealed binding affinities to heparin/HSPGs in the high nanomolar range and dependence on calcium. Both 3T3 mouse fibroblasts and human embryonic kidney cells (HEK-293) attached to PCPE-1, an interaction that was inhibited by heparin. Cell attachment was also inhibited by an NTR-specific antibody and the NTR fragment. Immunofluorescence analysis revealed that PCPE-Flag binds to mouse fibroblasts and heparin competes for this binding. Cell-associated PCPE-Flag stimulated procollagen processing by BMP-1 several fold. Our data suggest that through interaction with cell surface HSPGs, the NTR domain can anchor PCPE-1 to the cell membrane, permitting pericellular enhancement of PCP activity. This points to the cell surface as a physiological site of PCPE-1 action.

Fibrillar procollagen precursors contain N- and C-terminal propeptide extensions at both ends of their pro α chains. These propeptides must be removed for proper collagen fibril assembly to occur (1). The C-propeptide is removed by procollagen C-proteinases (PCPs),² a number of closely related tolloid fam-

ily metalloproteinases that play important regulatory roles in developmental processes and extracellular matrix assembly. This functional versatility results from their ability to process a variety of matrix components in addition to fibrillar procollagens, including non-fibrillar procollagens, small leucine-rich proteoglycans, growth factors (e.g. growth differentiation factors 8 and 11), and associated regulatory proteins (chordin, latent TGF- β -binding protein) and lysyl oxidases, enzymes responsible for elastin and collagen cross-linking (reviews in Refs. 2, 3). Procollagen processing by bone morphogenetic protein-1 (BMP-1), the prototype and apparently most active PCP (3, 4), can be stimulated by procollagen C-proteinase enhancers-1 and 2 (PCPE-1 and -2), two extracellular matrix glycoproteins lacking proteolytic activity of their own (5–8). Enhancement of BMP-1 activity by PCPE-1 appears to be restricted to fibrillar procollagen precursors because PCPE-1 does not affect BMP-1 activity on other tolloid substrates (9).

PCPE-1 is abundant in connective tissues rich in collagen I and in fibrotic tissues where it functions as a positive regulator of collagen deposition (6, 10). Increased expression of PCPE-1 in both liver (11) and cardiac fibrosis (12, 13) points at PCPE-1 as a potential therapeutic target in fibrosis. PCPE-1 expression is also increased in cultured smooth muscle cells and in intimal thickening induced by arterial injury. It may thus play a role in the proliferation of smooth muscle cells and extracellular matrix production during atheroma formation (14). The other procollagen C-proteinase enhancer, PCPE-2, has a much more limited distribution of expression than PCPE-1 (8).

PCPE-1 consists of two CUB domains that bind to the procollagen C-propeptide and are required for enhancing activity (6, 15) followed by a C-terminal NTR (netrin-like) domain (16) that binds to heparin (17) and as was recently demonstrated (18), also interacts with BMP-1. The NTR domain of PCPE-1 also binds to β 2-microglobulin, which may help initiate β 2-microglobulin amyloid fibril formation in connective tissues (19). The CUB and NTR domains in PCPE-1 are separated by two linkers: a short linker (9 amino acids in human PCPE-1)

* This work was supported by the GIS Maladies Rares INSERM Grant A041155P (to S. R.-B.), the Israel Science Foundation (Grants 736/01 and 1360/07), the European Commission (Contract No. NMP2-CT-2003-504017), and the Tel Aviv University Sackler Faculty of Medicine Maratier and Gothelf Foundations (to E. K.).

¹ To whom correspondence should be addressed. Tel.: 972-3-5350392; Fax: 972-3-5351577; E-mail: ekessler@post.tau.ac.il.

² The abbreviations used are: PCP, procollagen C-proteinase; BAPTA, cal-

cium chelator 1,2-bis-(2-aminophenoxy)ethane-*N,N,N',N'*-tetraacetic acid; BMP-1, bone morphogenetic protein-1; CUB, module found in complement subcomponents C1r/C1s, Uegf, and BMP-1; ECM, extracellular matrix; HP, heparin; HS, heparan sulfate; HEK, human embryonic kidney; NTR, netrin-like; PEG, polyethylene glycol; PCPE, procollagen C-proteinase enhancer; RU, resonance unit; SPR, surface plasmon resonance; TLCK, *N*^ε-tosyl-L-lysine chloromethyl ketone; TPCK, *N*-*p*-tosyl-L-phenylalanine chloromethyl ketone.

PCPE-1 Binding to Heparin/Heparan Sulfate

between the two CUB domains and a long linker (44 amino acids in human PCPE-1) that is sensitive to proteolysis between the second CUB and the NTR domain (6, 19, 20). The NTR domain has homology with the N-terminal domain of tissue inhibitors of metalloproteinases and with the C-terminal domain of netrins, complement components C3, C4, and C5, and secreted frizzled-related proteins (16). The NTR fragment of PCPE-1 has been reported to act as a weak inhibitor of matrix metalloproteinases (21). However, no inhibitory activity was detected by other investigators against a range of metalloproteinases, including MMPs-1, -2, -3, and -9, BMP-1 and different ADAMTS proteinases (18, 22). The PCPE-1 molecule has been shown to be a rod-like molecule, with a length of ~15 nm (23). The short linker between the CUB domains of PCPE-1 provides a flexible tether linking two binding sites within the individual CUB domains that act cooperatively in the binding of PCPE-1 to the procollagen substrate (20).

PCPE-1 binding to heparin suggests that PCPE-1 may also interact with heparan sulfate proteoglycans (HSPGs). HSPGs carry out distinct biological functions, from maintenance of basement membrane homeostasis to modulation of growth factor activity and angiogenesis (24). They are abundant at cell surfaces and within the extracellular matrix and heparan sulfate (HS) is a complex and highly active biopolymer, which binds to a wide variety of growth factors, morphogens, chemokines, and extracellular matrix proteins (25–27). HSPGs act as co-receptors for several tyrosine kinase receptors and have been shown to be important in controlling the biological activities of the bound factor (26). In this study, using surface plasmon resonance (SPR) binding assays, we characterized at the molecular level the binding of PCPE-1 to heparin and heparan sulfate, which is likely to be the physiological partner of PCPE-1. This included determination of the kinetics and affinity constants and demonstration of the role of divalent cations in this interaction. We have also investigated the role of this interaction in mediating cell adhesion to PCPE-1 and in anchoring PCPE-1 to the cell membrane, revealing that cell-bound PCPE-1 can augment procollagen processing by BMP-1 at the cell surface. The binding of PCPE-1 to heparan sulfate might play a major role in the assembly of the molecular machines comprised of bone morphogenetic protein-1, PCPE-1, and procollagens, which ensure the processing of procollagen molecules at the cell surface.

EXPERIMENTAL PROCEDURES

Construction of an Expression Vector for Recombinant Human PCPE-1-Flag Production—The full-length cDNA for human PCPE-1 (1474 bp) was excised from clone KT11 in pBlueSkriptII KS (6) and was ligated into the EcoRI site of pCDNA3.1(+) (Invitrogen). The Flag peptide coding sequence was inserted following the NTR domain coding sequence using the forward primer 5'-ACTCCTCGTCCAGTTCGTCTCAG-ATCTCAGTGTCA-3' (containing a BspEI site for cloning) and the reverse primer 5'-TTATACTCGAGTCACTTGTC-GTCGTCCTTGTAGTCGTCCTGGGACGCAGCAGCCCGCAC-3' (containing the Flag sequence and XhoI site for cloning). A PCR fragment (587 bp) was generated and ligated between the BstXI and EcoRI sites of the pcDNA3.1(+)

PCPE-1. Correct insertion of the sequences was verified by DNA sequencing of the insert-vector junctions.

Generation of Stable HEK-293 EBNA Clones Expressing PCPE-1 Flag—HEK-293 EBNA-1 cells (Invitrogen) were cultured in DMEM containing 10% (v/v) fetal calf serum at 37 °C in a humidified 5% CO₂ atmosphere. Transient transfection with the pCDNA3.1 plasmid bearing the coding sequence for PCPE-1 Flag was carried out with Lipofectamine 2000 (Invitrogen) according to the manufacturer's instructions. Stable clones expressing PCPE-1 Flag were isolated by selection with neomycin.

Protein Production and Purification—Human recombinant PCPE-1 was produced in 293-EBNA cells harboring the pCEP4 plasmid bearing the cDNA for PCPE-1 (provided by Dr. D. Hulmes) and purified from conditioned medium as previously described (9, 17). The NTR fragment was generated by incubating 2 mg of PCPE-1 (10 mg/ml in 50 mM Hepes, 150 mM NaCl, 5 mM CaCl₂, pH 7.4; buffer A) with trypsin (1:50 w/w; TPCK-treated; Sigma) for 30 min at room temperature. The reaction was stopped with TLCK (5 mM; Sigma), and the NTR fragment was separated from the CUB1CUB2 fragment by chromatography on a 5-ml HiTrapTM Heparin HP column (Amersham Biosciences, now GE Healthcare). The CUB1CUB2 fragment was recovered in the flow-through fractions and the bound NTR fragment was eluted with a linear gradient of NaCl (50 ml; 0.15–1 M NaCl in buffer A). Purity of the proteins was ascertained by SDS-PAGE on 12% gels and Coomassie staining. Three NTR fragments migrating closely at ~20 kDa were detected. Based on N-terminal sequencing, the major one with intermediate mobility, resulted from cleavage at the Lys²⁹⁹—Ser³⁰⁰ peptide bond (positions in pre-human PCPE-1) within the protease-sensitive CUB2-NTR linker.

Flag-tagged recombinant human PCPE-1 was expressed in 293-EBNA cells harboring the pCDNA3.1 plasmid bearing the PCPE-1 Flag construct and purified by Affi-blue and HiTrapTM heparin chromatography, as was used for PCPE-1 purification (17), followed by chromatography on an anti-Flag-antibody-Sepharose column (Sigma), to separate PCPE-1 Flag from small amounts of endogenous PCPE-1 secreted by HEK-293 cells. Bound PCPE-1 Flag was eluted from the column using the Flag peptide following the manufacturer's instructions.

Cell Attachment Assay—NIH 3T3 mouse fibroblasts and HEK-293 EBNA cells were grown (37 °C; 7% CO₂) in high glucose DMEM (Biological Industries, Bet Ha'emek, Israel) supplemented with 10% fetal calf serum (FCS), 2 mM glutamine, 100 units/ml penicillin, and 100 μg/ml streptomycin.

PCPE-1 (250 μg) was biotinylated using NHS-EZ-link biotin (Pierce; 10 μg in 500 μl of buffer A; 60 min at 4 °C). The reaction was stopped by adding 0.1 M NH₄Cl (35 μl) for 30 min, followed by dialysis against buffer A to remove the reagents. PCPE-1 activity was then determined (4, 15) to ensure that the modification did not affect its enhancing activity.

For the cell attachment assay, wells in 96-well plates were coated with extravidin (2 μg/ml in 0.1 M NaHCO₃, pH 8.3; overnight at 4 °C). After washing with TBS, the wells were blocked with 2% BSA in TBS + 5 mM CaCl₂ for 2 h at room temperature and biotin-PCPE-1 (50 ng/ml in blocking buffer; 50 μl) was

then added and allowed to bind to the extravidin-coated wells for 30 min at room temperature.

3T3 mouse fibroblasts or HEK-293 EBNA cells from fresh cultures were dissociated with 5 mM EDTA, washed with and resuspended in serum-free DMEM at 600,000 cells/ml. 100 μ l of the cell suspension (6×10^4 cells) were then added to each well, and the cells were allowed to attach to PCPE-1 for 45 min. After washing, attached cells were fixed for 30 min with glutaraldehyde (5%) and stained overnight with 0.1% crystal violet. Excess dye was removed by washing, the stained cells were then lysed with 10% acetic acid and absorbance at 595 nm was determined using an ELISA reader (28). For inhibition studies, increasing amounts of heparin (low mol wt; Sigma H3400) or a monoclonal antibody (IgG fraction) recognizing the NTR domain (7A11/5; Santa Cruz) or murine immunoglobulins (Sigma) as a negative control, were allowed to bind to the PCPE-1 coated wells for 2 h before addition of the cell suspension. In another set of inhibition experiments, the cells were preincubated with or without various concentrations of the NTR fragment before attachment to biotinylated PCPE-1.

Immunofluorescence Analysis—3T3 mouse fibroblasts were grown on coverslips as above except that 48 h before the experiment, the medium was supplemented with sodium ascorbate (50 μ g/ml) and 24 h before the experiment, the cells were placed on serum-free medium containing ascorbate. After washing, PCPE-1 Flag (200 ng/ml) in the same medium was added and incubated with the cells for 2 h at 37 °C to allow binding. Excess PCPE-Flag was removed by washing with PBS + 0.05% Tween-20. The cells were then fixed with 3.7% paraformaldehyde in PBS for 10 min, blocked with 10% FCS in PBS + 0.05% Tween 20 for 2 h, followed by incubation (2 h) with a rabbit antibody against the Flag peptide (Sigma, IgG fraction; 5 μ g/ml in blocking buffer). The cells were finally probed with a goat anti rabbit IgG antibody coupled to Cy2 in the presence of DAPI for 1 h in the dark. Fluorescence at 405 nm (DAPI) and 510 nm (Cy2) was detected using a fluorescence microscope (Olympus BX51).

Enhancement of PCP Activity by Cell-bound PCPE-Flag—3T3 mouse fibroblasts were inoculated into 35 mm tissue culture plates (Nunc) at a density of 1.2×10^4 cells/cm² and grown as above. At 70% confluence, the cells were placed on fresh medium containing sodium ascorbate (50 μ g/ml) and incubated further for 16 h. After washing, the cells were placed on serum-free medium containing ascorbate for additional 24 h. The cells were then washed again and incubated in serum-free DMEM containing various concentrations of PCPE-Flag (0, 50, 100, 200 ng/ml, as indicated) for 90 min to allow PCPE-Flag binding to the cells. Excess PCPE-Flag was removed by washing and the cells were then incubated for 2 h with [³H]tryptophan labeled chick embryo procollagen type I (15) (5 μ g; 140,000 cpm; in 1 ml of 50 mM Hepes, 150 mM NaCl, 5 mM CaCl₂, pH 7.5 containing 0.1% BSA and 4% PEG (mol wt 4,000 Da; Sigma) to allow deposition on the cell surface of the procollagen substrate. Excess procollagen was removed by washing with the above buffer, and purified recombinant human BMP-1 (0, 0.025, 0.1, or 0.2 units) expressed in HEK-293 cells (9) was then added in 1 ml of the same buffer, and the cells were incubated for 2 h at 37 °C for procollagen processing to occur. The super-

natants containing the free C-propeptide were collected, and the cell layers were washed and solubilized in 100 μ l of PBS containing 1 μ g/ml leupeptin (Sigma), 1 μ g/ml aprotinin (Roche), 1 mM PMSF, 1 mM 1,10-phenanthroline, and 2% SDS. The amount of radioactivity in each fraction was determined using a Packard model 1600 CA β -counter. Radioactive proteins were identified by SDS-PAGE followed by autoradiography. Proteins in the supernatants were concentrated 10-fold before separation by SDS-PAGE using TCA precipitation. The amount of PCPE-Flag in the various fractions was assessed by immunoblotting using a rabbit anti-Flag antibody and an horseradish peroxidase-coupled goat antirabbit IgG as a secondary antibody (both from Sigma), and ECL detection.

Surface Plasmon Resonance Binding Assays—The SPR measurements were performed on a BIAcore 3000 instruments (GE Healthcare). Streptavidin (100 μ g/ml in 10 mM acetate buffer, pH 4.0) was covalently immobilized to the dextran matrix of a CM4 sensor chip *via* its primary amine groups (amine coupling kit, GE Healthcare) at a flow rate of 5 μ l/min. Activation and blocking steps were performed as described previously (29–31). Streptavidin surfaces were used to capture heparin and heparan sulfate from porcine intestinal mucosa, which were biotinylated at their reducing end (30). Glycosaminoglycans were injected over streptavidin in 10 mM Hepes, pH 7.4, 0.3 M NaCl, and 0.005% P20 surfactant at a flow rate of 10 μ l/min. An immobilization level ranging between 100 and 250 resonance units (RU) was obtained. A control flow cell was prepared by injecting biotin-LC hydrazide over immobilized streptavidin. Control sensorgrams were automatically subtracted from the sensorgrams obtained on immobilized heparin or heparan sulfate to yield true binding responses. Binding assays were performed at 25 °C in 10 mM Hepes buffer, pH 7.4, containing 0.15 M NaCl, 0.005% (v/v) P20 surfactant (HBS-P buffer, GE Healthcare) and 5 mM CaCl₂. PCPE-1 and the NTR domain were injected at 30 μ l/min for 4 min over immobilized glycosaminoglycans. The complexes formed by PCPE-1 and heparin/heparan sulfate were dissociated upon injection of a mixture of 1 M sodium chloride and 1.5 M guanidinium chloride.

The kinetic parameters k_a and k_d (association and dissociation rate constants, respectively) were analyzed simultaneously using a global data analysis program (BIAevaluation 3.1 Software). This software fitted simultaneously the sensorgrams obtained at different concentrations of PCPE-1 (7–1000 nM) and of the NTR domain (161–2580 nM) constraining the kinetic rate constants to a single value for each set of curves. Apparent equilibrium dissociation constants (K_D) were calculated as the ratio of k_d/k_a . The maximal capacity of the surface (R_{max}) was floated during the fitting procedure. The χ^2 value, a standard statistical measure of the closeness of fit, which represents the mean square of the signal noise (BIAevaluation 3.0 Software Handbook) was calculated.

For inhibition experiments, PCPE-1 (1 μ M) and the NTR domain (1.3 μ M) were preincubated with 5 μ g/ml glycosaminoglycans or carboxy-methyl-dextran for 1 h at room temperature prior to injection over immobilized heparin or heparan sulfate. Chondroitin sulfate from bovine trachea (C8529), heparin (H3393), and dermatan sulfate (C3788) from porcine intestinal

PCPE-1 Binding to Heparin/Heparan Sulfate

TABLE 1

Kinetics and affinity values

Kinetics and affinity values were calculated using the BIAeval 3.0 software for the binding of the NTR domain of PCPE-1 with heparin ($n = 2$), heparan sulfate ($n = 4$), and with full-length PCPE-1 with heparin ($n = 1$) and heparan sulfate ($n = 2$). Data were fitted by the 1:1 Langmuir model.

Immobilized molecule	Injected molecule	k_a $M^{-1}s^{-1}$	k_d s^{-1}	K_D M
Heparin	NTR domain	$1.45 \times 10^3 \pm 1 \times 10^1$	$1.09 \times 10^{-4} \pm 7.5 \times 10^{-6}$	$7.57 \times 10^{-8} \pm 4.5 \times 10^{-9}$
Heparan sulfate	NTR domain	$3.11 \times 10^3 \pm 6.70 \times 10^2$	$9.03 \times 10^{-5} \pm 1.28 \times 10^{-5}$	$3.13 \times 10^{-8} \pm 1.08 \times 10^{-8}$
Heparin	PCPE-1	6.05×10^3	3.82×10^{-4}	6.32×10^{-8}
Heparan sulfate	PCPE-1	$3.67 \times 10^3 \pm 1.00 \times 10^3$	$4.53 \times 10^{-4} \pm 1.44 \times 10^{-4}$	$1.22 \times 10^{-7} \pm 1.55 \times 10^{-8}$

mucosa were from Sigma-Aldrich. Heparan sulfate from porcine intestinal mucosa was from Celsus (Cincinnati, OH).

The dependence of the binding upon cations was investigated by adding EDTA, a chelator of several divalent cations including Zn^{2+} , Mg^{2+} , or Ca^{2+} , and BAPTA, a selective calcium chelator, in the solutions of PCPE-1 and of the NTR domain before their injection over immobilized glycosaminoglycans. The three-dimensional structure of the NTR domain of human PCPE-1 (22, 32) was used to predict binding site(s) of heparin on the NTR domain.

RESULTS

Characterization of the Binding of PCPE-1 to Heparin/Heparan Sulfate—The binding of PCPE-1 to heparin was characterized at the molecular level by SPR binding assays. Highly sulfated heparin is a model for heparan sulfate and is used in the vast majority of the interaction studies with proteins. Heparan sulfate is much less substituted with sulfate groups than heparin and has a more varied structure (25). The physiological ligands of proteins, either at the cell surface or in the extracellular matrix, being heparan sulfate, we analyzed the binding of PCPE-1 both to heparin and heparan sulfate.

PCPE-1 was injected at several concentrations over immobilized heparin and heparan sulfate. Kinetic data were fitted by the Langmuir binding model (one PCPE molecule binds to one heparin or heparan sulfate molecule). The affinity of the PCPE-1 molecule was higher for heparin (~63 nM) than for heparan sulfate (~122 nM, Table 1). The complexes formed by PCPE-1 and glycosaminoglycans were of moderate stability. Kinetic data were also well fitted by the heterogeneous ligand model, suggesting that one PCPE-1 molecule could bind independently to two sites on immobilized glycosaminoglycans. The affinities of PCPE-1 for the two binding sites were $K_{D1} \sim 81$ nM and $K_{D2} \sim 32.5$ nM for heparin and $K_{D1} \sim 88$ nM and $K_{D2} \sim 300$ nM for heparan sulfate. The existence of two binding sites can be explained by the natural heterogeneity of heparin and heparan sulfate. Both glycosaminoglycans undergo extensive modification after the initial polymer synthesis, and binding to subpopulations of glycosaminoglycans may occur. Indeed we have previously shown that kinetic data of the binding of endostatin, the C-terminal domain of collagen XVIII (30) and of HepV, a fragment of collagen V (31), to heparin/heparan sulfate were well fitted by a heterogeneous ligand model.

PCPE-1 binding to heparin is mediated by the NTR domain (17, 18). Therefore, we have also characterized the binding of the free NTR domain of PCPE-1 to heparin and heparan sulfate. As expected, the NTR domain alone bound to heparin and to heparan sulfate (Fig. 1). Kinetic data were best fitted to the

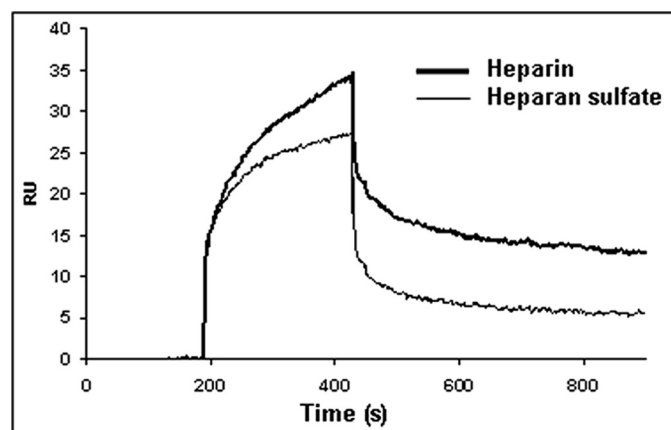


FIGURE 1. Binding of the NTR domain of PCPE-1 (645 nm) to immobilized heparin (154 RU) and heparan sulfate (175 RU). Flow rate: 30 μ l/min, contact time: 4 min, sample buffer: HBS-P + 5 mM $CaCl_2$.

TABLE 2

Inhibition (expressed as percentage of binding in the absence of competitor) of the binding of PCPE-1 and of the NTR domain to immobilized heparin or heparan sulfate by various glycosaminoglycans (5 μ g/ml)

Glycosaminoglycan added	Immobilized heparin		Immobilized heparan sulfate	
	PCPE-1	NTR domain	PCPE-1	NTR domain
Heparin	95.87	97.75	95.06	100.42
Heparan sulfate	73.15	45.46	76.45	65.47
Dermatan sulfate	45.09	4.83	45.06	14.95

Langmuir model (one NTR domain binds to one heparin or heparan sulfate molecule). The affinity of the NTR domain was lower for heparin (~76 nM) than for heparan sulfate (~31 nM, Table 1). Kinetic data were also well fitted by the heterogeneous ligand model indicating that one NTR domain might bind independently to two sites on immobilized glycosaminoglycans. In this model the affinity of the NTR domain for the two heparin binding sites was $K_{D1} \sim 67$ nM and $K_{D2} \sim 27$ nM for heparin and $K_{D1} \sim 12$ nM and $K_{D2} \sim 15.5$ nM for heparan sulfate. Thus, the NTR domain bound to heparan sulfate with a higher affinity than full-length PCPE-1.

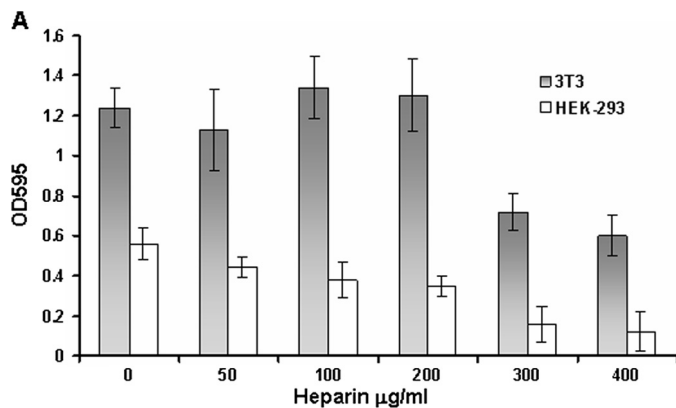
Preincubation of PCPE-1 and the NTR domain with heparin nearly abolished their binding to heparin and heparan sulfate (Table 2). Heparan sulfate also inhibited the binding of PCPE-1 and of the NTR domain to both glycosaminoglycans by up to 76%. Dermatan sulfate inhibited the binding of full-length PCPE-1 to immobilized heparin and heparan sulfate by 45%, but inhibited poorly (less than 15%) the binding of the NTR domain to the immobilized glycosaminoglycans (Table 2). Chondroitin sulfate and carboxymethyl-dextran, which is a polyanion lacking sulfate groups, failed to inhibit

the binding of PCPE-1 and of the NTR domain to heparin and heparan sulfate (not shown). This confirms that sulfate groups play a major role in the binding of heparin/heparan sulfate to PCPE-1/NTR.

TABLE 3

Inhibition (expressed as percentage of binding in the absence of ion chelator) of the binding of PCPE/NTR to immobilized glycosaminoglycans in the presence of 20 mM EDTA or 20 mM BAPTA

Injected molecule	Immobilized heparin		Immobilized heparan sulfate	
	PCPE-1	NTR	PCPE-1	NTR
20 mM EDTA	63.1	57.2	60.4	47.4
20 mM BAPTA	96.8	97.5	89.7	90.8



B

Cells	3T3	HEK-293
Heparin (µg/ml)	Binding (%) ± S.D.	
0	100 ± 8.5	45 ± 9.3
50	91 ± 6	35 ± 8.8
100	108 ± 7.3	31 ± 5.3
200	105 ± 10	28 ± 6
300	58 ± 6	13 ± 4
400	48 ± 5	9.6 ± 3

FIGURE 2. Heparin inhibits attachment of 3T3 mouse fibroblasts and HEK-293 cells to PCPE-1. A, cell attachment to PCPE-1 in the absence or presence of increasing concentrations of heparin (0–400 µg/ml); B, cell binding to PCPE-1 expressed as percentage of binding of 3T3 mouse fibroblasts in the absence of heparin (100%). Each value represents mean ± S.D. (n = 4).

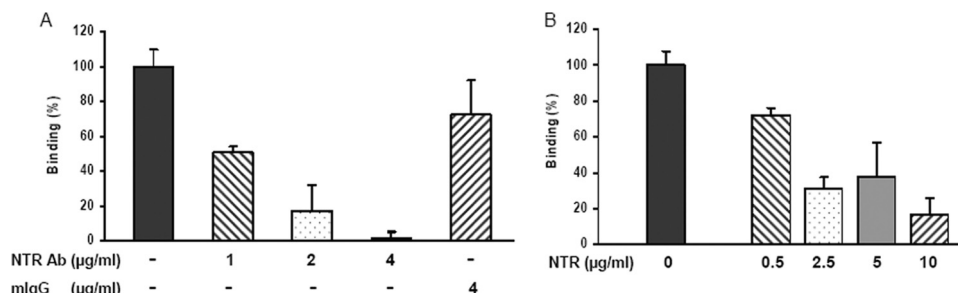


FIGURE 3. Attachment of 3T3 mouse fibroblasts to PCPE-1 is inhibited by a monoclonal antibody recognizing the NTR domain of PCPE-1 (A) and the free NTR fragment (B). A, biotin-labeled PCPE-1 was incubated with the anti-NTR mAb (1, 2, or 4 µg/ml) for 2 h prior to addition to extravidin-coated wells for adsorption. Normal murine immunoglobulin (mIgG; 4 µg/ml) served as a control. B, cells (60,000/100 µl) were incubated for 20 min with increasing concentrations (0.5–10 µg/ml) of the NTR domain before addition to the biotin-PCPE-1-coated wells. The cell attachment assay in both A and B, was then performed as described under “Experimental Procedures.” Each value represents mean ± S.D. (n = 4).

EDTA and BAPTA strongly inhibited the binding of PCPE-1 and its NTR domain to immobilized glycosaminoglycans (Table 3), indicating that the binding of PCPE-1 and the NTR domain to heparin/heparan sulfate depends upon divalent cations. BAPTA inhibited the binding to a higher extent than EDTA, suggesting that calcium ions participate in the binding.

Cell Adhesion to PCPE-1 Is Inhibited by Heparin—The binding of the NTR domain to heparan sulfate *in vitro* suggested it may bind to cell surface heparan sulfate proteoglycans *in vivo*. As a first step to examine this possibility, we tested whether cells can attach to PCPE-1 and if so, whether this interaction can be inhibited by heparin. We compared two cell types, 3T3 mouse fibroblasts as an example of cells that produce relatively high levels of both collagen type I and PCPE-1 and HEK-293 cells that do not express collagen and express low levels of PCPE-1. Both 3T3 mouse fibroblasts and HEK-293 cells attached to PCPE-1. The degree of attachment of 3T3 mouse fibroblasts was about twice as high as that of HEK-293 cells (Fig. 2). Heparin inhibited binding of both cell types to PCPE-1. The inhibition was dose-dependent for the HEK-293 cells and was higher than for 3T3 fibroblasts, reaching ~80% at the highest heparin concentrations tested (300–400 µg/ml; Fig. 2B). The binding and inhibition pattern seemed to be more complex for fibroblasts, with more efficient binding and an inhibition level limited to ~50% at the highest heparin concentrations tested (Fig. 2). These data suggested that while the attachment of both cell types involved a cell-surface proteoglycan(s), an additional cell-surface receptor might be involved in the adhesion of 3T3 mouse fibroblasts to PCPE-1. Alternatively, the amount of cell-surface proteoglycans acting as receptors on 3T3 mouse fibroblasts might be higher than on HEK 293 cells.

Cell Adhesion to PCPE-1 Is Mediated by Its C-terminal NTR Domain—A monoclonal antibody to the NTR domain strongly inhibited the attachment of 3T3 mouse fibroblasts to PCPE-1 (Fig. 3A). A normal mouse IgG used as a control did not cause significant inhibition. Furthermore, preincubation of cells with the NTR domain of PCPE-1 resulted in a decreased adhesion of these cells to PCPE-1 (Fig. 3B). These data clearly indicate that cell binding to PCPE-1 is largely mediated by its C-terminal NTR domain.

PCPE-1 Binding to Cells Is Inhibited by Heparin—The results of the cell attachment assay suggested that *in vivo*, PCPE-1 may bind to the cell membrane via a cell surface heparan sulfate proteoglycan(s). Using immunofluorescence localization as a tool, we examined whether exogenously added PCPE-1 Flag binds to 3T3 mouse fibroblasts and if so, whether heparin can displace the bound protein. Fig. 4 shows that PCPE-1 Flag binds to 3T3 mouse fibroblasts and that heparin competes for this binding in a dose-dependent manner. To achieve complete inhibition, prolonged incubation (6–16 h) with heparin was required. These results provide an additional evidence for the role of

PCPE-1 Binding to Heparin/Heparan Sulfate

the NTR domain in the interaction of PCPE-1 with cells. Furthermore, because the cells were not permeabilized, the data suggest that bound PCPE-1 was not internalized.

PCPE-1 Enhances C-terminal Procollagen Processing by BMP-1 on the Cell Surface—To explore the biological significance of PCPE-1 interaction with cells, we examined whether

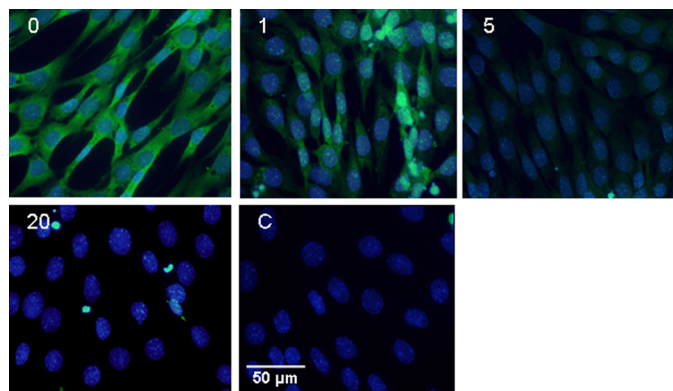


FIGURE 4. Heparin inhibits binding of PCPE-Flag to 3T3 mouse fibroblasts. Mouse fibroblasts at 70–80% confluency were incubated for 1.5 h with PCPE-Flag (200 ng/ml). Unbound PCPE-Flag was removed by washing with phosphate-buffered saline, and the cells were then placed on fresh medium supplemented with heparin (0, 1, 5, or 20 μ g/ml as indicated) and incubated further for 16 h (37 $^{\circ}$ C, 7% CO_2). The cells were then washed and fixed with 3.7% paraformaldehyde. Cell-bound PCPE-Flag was detected by immunofluorescence using an anti-Flag antibody and a Cy2-coupled secondary antibody. Nuclei were stained with DAPI. C, control: cells were incubated with PCPE-Flag without subsequent addition of heparin. Immunodetection was without addition of the first (anti-Flag) antibody.

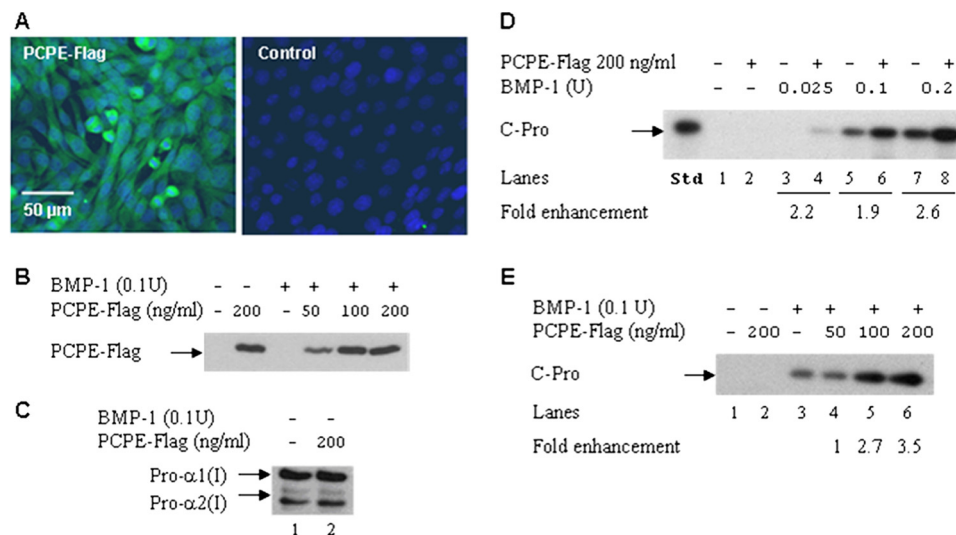


FIGURE 5. Cell-bound PCPE-Flag is maintained on the cell surface and stimulates procollagen processing by BMP-1 at this location. PCPE-Flag was allowed to bind to 3T3 mouse fibroblasts for 90 min. Radioactively labeled procollagen type I was then added and allowed to settle on the cells for additional 90 min. BMP-1 was then added, and the cells were incubated further for 2 h for procollagen processing to occur (total incubation time of 5 h). A, immunofluorescence analysis with an anti-Flag antibody (performed after 5 h of incubation with 200 ng/ml of PCPE-Flag) showing that PCPE-Flag remains cell-bound throughout the experiment. B, immunoblot of cell layer extracts prepared after 5 h of incubation and probed with an anti-Flag antibody, showing that the amount of cell-bound PCPE-Flag is proportional to the original input of PCPE-Flag. C, autoradiogram showing cell association of the procollagen substrate. Cells incubated without BMP-1 were solubilized, radioactivity was determined, and approximately half of the total cell-associated radioactivity (6,000 cpm) was loaded per lane. SDS-PAGE was performed on a 6% gel with reduction. Bands corresponding to the pro α 1(I) and pro α 2(I) chains are indicated by arrows. D, autoradiogram showing a comparable degree of enhancement of PCP activity (2–2.6-fold) at a constant input of PCPE-Flag (200 ng/ml), essentially independent of BMP-1 concentration. E, autoradiogram showing that the degree of enhancement of PCP activity, assessed by the C-propeptide release, increases as a function of PCPE-Flag concentration. Fold enhancement, ratio between the amount of radioactivity released into the supernatants in the presence and absence of PCPE-Flag, respectively.

cell-bound PCPE-Flag can stimulate C-terminal procollagen processing by BMP-1 on the cell surface. 3T3 mouse fibroblasts were incubated with PCPE-Flag followed by incubation with [^3H]tryptophan-labeled procollagen I to allow cell-surface localization of both. BMP-1 was then added and the cells were incubated further to permit procollagen processing. Maintenance of PCPE-Flag on the cell surface during the experiment (5 h) was verified by both immunofluorescence and immunoblotting analyses. Fig. 5A shows high fluorescence intensity (detected using an anti-Flag antibody) on cells incubated with 200 ng/ml of PCPE-Flag, indicating that much of the PCPE-Flag added to the cells was retained on their surface throughout the experiment. The immunoblotting analysis (Fig. 5B) also showed that PCPE-Flag remained cell associated for the duration of the experiment. Furthermore, the amount of cell-bound PCPE-Flag appeared to be proportional to the initial input of PCPE-Flag, with an apparent saturation at 100 ng/ml of PCPE-Flag. No PCPE-Flag was detected in the incubation solutions collected at the end of the experiment (not shown), further indicating that cell-bound PCPE-Flag was not released into the incubation medium, and its interaction with the cell membrane was durable. Similarly, in cells that were incubated either with procollagen alone or with procollagen and PCPE-Flag but without BMP-1, essentially all of the radioactivity (\sim 13,000 cpm) in the procollagen substrate that adsorbed to the cells remained cell-associated throughout the experiment (Fig. 5C). No radioactivity was released into the incubation solutions in the

absence of BMP-1 (not shown). Procollagen processing was followed by measuring the amount of radioactivity released into the incubation media and by SDS-PAGE and autoradiography to identify the reaction products (Fig. 5, D and E). We found that the only radioactive protein released into the incubation media was the free procollagen C-propeptide, and that in all instances, the amount of C-propeptide released in the presence of PCPE-Flag was higher than in its absence. When tested at increasing PCPE-Flag concentrations (Fig. 5E), the degree of enhancement of procollagen processing increased in a dose-dependent manner. Essentially no enhancement was observed upon addition of 50 ng/ml of PCPE-Flag (compare lanes 3 and 4), while the amount of C-propeptide released into the medium upon addition of 100 and 200 ng/ml of PCPE-Flag, increased 2.7- and 3.5-fold, respectively (lanes 5 and 6). When processing was followed as a function of BMP-1 concentration (at a constant PCPE-Flag concentration of 200 ng/ml), the degree of enhancement of procolla-

gen processing was comparable regardless of the BMP-1 input, ranging from 2–2.6-fold (compare lanes 3 and 4, 5 and 6, and 7 and 8 in Fig. 5D). Together, the results of this set of experiments indicate that the interaction of PCPE-Flag with cells is durable and that PCPE-1 can stimulate procollagen processing by BMP-1 when anchored to the cell membrane. These findings support our hypothesis that the interaction of the NTR domain with cell surface HSPGs plays a role in promoting procollagen processing at the cell surface.

DISCUSSION

In the present report, we found that PCPE-1 binds to heparin/heparan sulfate with an affinity in the high nanomolar range ($K_D = 63.2$ and 122 nM for heparin and heparan sulfate, respectively). This is lower than the affinity we have calculated for collagen I ($K_D = 3.4$ and 3.5 nM for heparin and heparan sulfate, respectively) and for collagen V ($K_D = 5.62$ and 2.0 nM for heparin and heparan sulfate, respectively (31), but much higher than the affinity of endostatin, a soluble fragment of collagen XVIII inhibiting angiogenesis ($K_D \sim 2$ μ M for both glycosaminoglycans) (30) or of the $\alpha 5\beta 1$ integrin (1.14 μ M and 2.04 μ M for heparin and heparan sulfate, respectively (33).

The strength of PCPE-1 binding to heparin has been previously evaluated by affinity chromatography on heparin-Sepharose. PCPE-1 eluted from the column between 0.4 and 0.5 M NaCl (17) or between 0.3 and 0.4 M NaCl (8). However, heparin-Sepharose may act as a cation exchanger because of the highly negative charge of heparin. The amount of salt required for elution of a protein from the affinity column is a quantitative measure of the ionic component of the binding, but fails to measure the hydrophobic and hydrogen bonding contributions to binding (25), whereas the SPR assays take into account all of the possible bonding mechanisms. Deviations between the relative ionic strength elution of proteins from heparin-Sepharose and direct affinity measurements have been observed (34), suggesting that differential ionic strength elution of proteins may not reflect their true relative affinities. The presence of two possible binding sites identified by fitting SPR kinetic data to the heterogeneous ligand model is in agreement with the fact that significant quantities of PCPE-1 eluted at NaCl concentrations lower than 0.3 M (8).

The NTR domain does not contain any of the three linear consensus sequences proposed for heparin binding (BBXB, BBXXB, and XBBBXXBBBXXBB, where B is a basic and X a hydrophobic, neutral and hydrophobic, amino acid residue (25). The precise binding site of heparin/heparan sulfate inside the NTR domain remains to be mapped. The three-dimensional structure of the NTR domain has been elucidated by NMR (22). It includes a patch with uncharged residues in the center and positive charges at the rim, including Lys³², Arg³⁶, Arg¹²⁰, Arg¹³⁴, Arg¹⁴⁷ (numbering of amino acid positions is as used in the NTR construct studied by Liepinsh *et al.* (22), in which position 30 corresponds to Cys³¹⁸ in full-length PCPE-1). Electrostatic surface representation of the NTR domain shows that several basic amino acids of the NTR domain are clustered on one face of the molecule, forming two other basic clusters that may bind heparin/heparan sulfate. The first one comprises Arg³⁵, Arg³⁶, and Arg¹⁴⁷ and the second one Lys¹⁰⁵, Lys¹⁰⁶,

Lys⁵⁶, Lys⁹⁹, and Arg⁶⁰. These basic clusters might also bind heparan sulfate.

The binding of PCPE-1/NTR to heparin/heparan sulfate requires divalent cations, and most likely calcium, as reported previously for other extracellular proteins such as endostatin (30), a fragment of collagen V (31), the $\alpha 5\beta 1$ integrin (33) and certain annexins (35). The role of calcium ions in the binding of the NTR domain of PCPE-1 to heparin is unclear. Based on its three-dimensional structure (22), this protein domain does not contain calcium ions. It is possible however that, as was shown for annexin A2 (35), some heparin binding sites may rely on calcium binding and not on arrays of basic residues. In this instance, main-chain and side chain nitrogen atoms and two calcium ions play an important role in the binding. Of special interest in this regard is the finding that a new calcium-binding site is formed in annexin A2 upon initial binding to heparin, in which two sugar residues within a small heparin derivative used as a model for heparin, provided oxygen ligands for this calcium ion. It is conceivable that a similar mechanism operates in the binding of the NTR domain to heparin, where initial binding to clusters of basic residues in the NTR domain may trigger the formation of a functionally important calcium binding site(s) for heparin.

Our data on the interaction of PCPE-1 with cells, including inhibition by heparin, a NTR-specific monoclonal antibody and the NTR fragment itself, strongly suggest that the NTR domain of PCPE-1 mediates the binding of PCPE-1 to cell surface HSPGs. This binding was observed with both HEK-293 cells that do not express collagen type I but express HSPGs and 3T3 mouse fibroblasts that produce and process relatively large amounts of procollagen I and also express HSPGs. The binding patterns and patterns of inhibition of cell attachment to PCPE-1 by heparin seen with these cell types were however different (Fig. 2). Higher cell binding and a lower degree of inhibition by heparin were seen with the fibroblasts as compared with the HEK-293 cells. This suggests that the interaction of PCPE-1 with fibroblasts may involve another receptor in addition to HSPGs, while the interaction of PCPE-1 with the HEK-293 cells was mainly mediated by HSPGs. Nonetheless, the interaction of the NTR domain with HSPGs seems to be cardinal for PCPE-1 binding to cells, as prolonged incubation of 3T3 mouse fibroblasts with heparin alone was sufficient to achieve complete displacement of PCPE-1 Flag from the cell surface. The finding that cell-bound PCPE-1 can be fully displaced by heparin (which does not penetrate intact cells) indicates that cell-bound PCPE-1 is not internalized, and suggests that PCPE-1 may function on the cell surface, accelerating procollagen processing at this location.

The biological significance of PCPE-1 interaction with heparan sulfate is not fully elucidated. To gain an insight on this question, we examined whether cell-bound PCPE-1 can stimulate PCP activity pericellularly. We used radioactively labeled procollagen and Flag-tagged PCPE-1 to facilitate their localization, and both were localized to the cell surface/cell layer during enzymatic processing by BMP-1. The results of the processing assays, which were performed with and without addition of PCPE-Flag, document for the first time cell-associated enhancing activity of PCPE-1. This suggests the cell surface as a phys-

PCPE-1 Binding to Heparin/Heparan Sulfate

iological site of PCPE-1 enhancing activity, and is in agreement with previous reports indicating that in tendon, fibrillogenesis is initiated in a series of extracellular compartments defined by the fibroblasts and close to their surface (36).

The highest degree of enhancement (3.5-fold) was however lower than that obtained in the standard assay of PCP activity (~10-fold) that is performed in solution at optimal (1:1) molar ratios of PCPE-1 and procollagen (29). This could be due to the fact that in the cell-based assay, we only measured an increment in enhancing activity, above that provided by endogenous PCPE-1, which also binds to the cell membrane and can be displaced from it by heparin (37).

The interaction of the NTR domain with heparan sulfate seems to play a role in anchoring PCPE-1 to the cell membrane where it can take part in the processing of a number of extracellular matrix proteins by BMP-1, including fibrillar procollagen precursors. Assembly of functional multiprotein complexes has been reported on the heparan sulfate polymer chain (27). Heparan sulfate may act as a guiding scaffold to bring BMP-1, PCPE-1, and procollagen molecules together in areas of collagen fibrillogenesis, playing a pivotal role in the building of the molecular machines involved in procollagen processing. Indeed, heparan sulfate chains bind with moderate affinity to PCPE-1, which is required to enhance BMP-1 activity, to procollagen I with high affinity in the nanomolar range (31), and transiently to BMP-1 with low affinity in the micromolar range (0.5–2 μM) (18). Once the complexes are anchored at the cell surface via several proteins, rearrangements could occur, and some PCPE-1 molecules could bind to BMP-1 via their NTR domain (18). The functional importance of complexes assembled by heparan sulfate is highlighted by the recent demonstration that heparin/heparan sulfate can increase the enhancing activity of PCPE-1 further (about 2-fold) in the processing of (mini) procollagen III by BMP-1, an effect described as “super-stimulation” of PCPE-1 (18). Similar complexes can be formed during the processing of pro- $\alpha 1(\text{V})$ N-propeptides and pro- $\alpha 2(\text{V})$ C-propeptides by BMP-1-like enzymes (38). Finally, PCPE-2 may also function as a component of such a multimolecular complex because, similarly to PCPE-1, it binds to heparin and there is evidence indicating that much of the PCPE-2 antigen is found pericellularly (8).

REFERENCES

1. Ricard-Blum, S., Ruggiero, F., and van der Rest, M. (2005) *Top. Curr. Chem.* **247**, 35–84
2. Kessler, E. (2004) in *Handbook of Proteolytic Enzymes* (2nd Ed.) (Barrett, A. J., Rawlings, N. D., and Woessner, J. F., eds) Vol. 1, pp. 609–617, Elsevier, Academic Press
3. Hopkins, D. R., Keles, S., and Greenspan, D. S. (2007) *Matrix Biol.* **26**, 508–523
4. Kessler, E., Takahara, K., Biniaminov, L., Brusel, M., and Greenspan, D. S. (1996) *Science* **271**, 360–362
5. Adar, R., Kessler, E., and Goldberg, B. (1986) *Coll. Relat. Res.* **6**, 267–277
6. Takahara, K., Kessler, E., Biniaminov, L., Brusel, M., Eddy, R. L., Jani-Sait, S., Shows, T. B., and Greenspan, D. S. (1994) *J. Biol. Chem.* **269**, 26280–26285
7. Xu, H., Acott, T. S., and Wirtz, M. K. (2000) *Genomics* **66**, 264–273
8. Steiglitz, B. M., Keene, D. R., and Greenspan, D. S. (2002) *J. Biol. Chem.* **277**, 49820–49830
9. Moali, C., Font, B., Ruggiero, F., Eichenberger, D., Rousselle, P., François, V., Oldberg, A., Bruckner-Tuderman, L., and Hulmes, D. J. (2005) *J. Biol. Chem.* **280**, 24188–24194
10. Kessler, E., Mould, A. P., and Hulmes, D. J. (1990) *Biochem. Biophys. Res. Commun.* **173**, 81–86
11. Ogata, I., Auster, A. S., Matsui, A., Greenwel, P., Geerts, A., D'Amico, T., Fujiwar, K., Kessler, E., and Rojkind, M. (1997) *Hepatology* **26**, 611–617
12. Shalitin, N., Schlesinger, H., Levy, M. J., Kessler, E., and Kessler-Icekson, G. (2003) *J. Cell. Biochem.* **90**, 397–407
13. Kessler-Icekson, G., Schlesinger, H., Freimann, S., and Kessler, E. (2006) *Int. J. Biochem. Cell Biol.* **38**, 358–365
14. Kanaki, T., Morisaki, N., Bujo, H., Takahashi, K., Ishii, I., and Saito, Y. (2000) *Biochem. Biophys. Res. Commun.* **270**, 1049–1054
15. Kessler, E., and Adar, R. (1989) *Eur. J. Biochem.* **186**, 115–121
16. Bányai, L., and Patthy, L. (1999) *Protein Sci.* **8**, 1636–1642
17. Moschovich, L., Bernocco, S., Font, B., Rivkin, H., Eichenberger, D., Chejanovsky, N., Hulmes, D. J., and Kessler, E. (2001) *Eur. J. Biochem.* **268**, 2991–2996
18. Bekhouche, M., Kronenberg, D., Vadon-Le Goff, S., Bijakowski, C., Lim, N. H., Font, B., Kessler, E., Colige, A., Nagase, H., Murphy, G., Hulmes, D. J., and Moali, C. (2010) *J. Biol. Chem.* **285**, 15950–15959
19. Morimoto, H., Wada, J., Font, B., Mott, J. D., Hulmes, D. J., Ookoshi, T., Naiki, H., Yasuhara, A., Nakatsuka, A., Fukuoka, K., Takatori, Y., Ichikawa, H., Akagi, S., Nakao, K., and Makino, H. (2008) *Matrix. Biol.* **27**, 211–219
20. Kronenberg, D., Vadon-Le Goff, S., Bourhis, J. M., Font, B., Eichenberger, D., Hulmes, D. J., and Moali, C. (2009) *J. Biol. Chem.* **284**, 33437–33446
21. Mott, J. D., Thomas, C. L., Rosenbach, M. T., Takahara, K., Greenspan, D. S., and Banda, M. J. (2000) *J. Biol. Chem.* **275**, 1384–1390
22. Liepinsh, E., Banyai, L., Pintacuda, G., Trexler, M., Patthy, L., and Otting, G. (2003) *J. Biol. Chem.* **278**, 25982–25989
23. Bernocco, S., Steiglitz, B. M., Svergun, D. I., Petoukhov, M. V., Ruggiero, F., Ricard-Blum, S., Ebel, C., Geourjon, C., Deleage, G., Font, B., Eichenberger, D., Greenspan, D. S., and Hulmes, D. J. (2003) *J. Biol. Chem.* **278**, 7199–7205
24. Iozzo, R. V., Zoeller, J. J., and Nyström, A. (2009) *Mol. Cells* **27**, 503–513
25. Capila, I., and Linhardt, R. J. (2002) *Angew. Chem. Int. Ed. Engl.* **41**, 391–412
26. Whitelock, J. M., and Iozzo, R. V. (2005) *Chem. Rev.* **105**, 2745–2764
27. Gallagher, J. T. (2006) *Biochem. Soc. Trans.* **4**, 438–441
28. Humphries, M. J. (2001) *Mol. Biotechnol.* **18**, 57–61
29. Ricard-Blum, S., Bernocco, S., Font, B., Moali, C., Eichenberger, D., Farjanel, J., Burchardt, E. R., van der Rest, M., Kessler, E., and Hulmes, D. J. (2002) *J. Biol. Chem.* **277**, 33864–33869
30. Ricard-Blum, S., Féraud, O., Lortat-Jacob, H., Rencurosi, A., Fukai, N., Dkhissi, F., Vittet, D., Imbert, A., Olsen, B. R., and van der Rest, M. (2004) *J. Biol. Chem.* **279**, 2927–2936
31. Ricard-Blum, S., Beraud, M., Raynal, N., Farndale, R. W., and Ruggiero, F. (2006) *J. Biol. Chem.* **281**, 25195–25204
32. Williamson, R. A., Panagiotidou, P., Mott, J. D., and Howard, M. J. (2008) *Mol. Biosyst.* **4**, 417–425
33. Faye, C., Moreau, C., Chautard, E., Jetne, R., Fukai, N., Ruggiero, F., Humphries, M. J., Olsen, B. R., and Ricard-Blum, S. (2009) *J. Biol. Chem.* **284**, 22029–22040
34. Powell, A. K., Yates, E. A., Fernig, D. G., and Turnbull, J. E. (2004) *Glycobiology* **14**, 17R–30R
35. Shao, C., Zhang, F., Kemp, M. M., Linhardt, R. J., Waisman, D. M., Head, J. F., and Seaton, B. A. (2006) *J. Biol. Chem.* **281**, 31689–31695
36. Zhang, G., Young, B. B., Ezura, Y., Favata, M., Soslowsky, L. J., Chakravarti, S., and Birk, D. E. (2005) *J. Musculoskelet. Neuronal Interact.* **5**, 5–21
37. Wineman, E., Weiss, T., Farzam, N., Savion, N., Smorodinsky, I. N., and Kessler, E. (2008) *Federation of the European Connective Tissue Societies, Marseille, France, July 9–13, 2008, Federation of the European Connective Tissue Societies*
38. Unsöld, C., Pappano, W. N., Imamura, Y., Steiglitz, B. M., and Greenspan, D. S. (2002) *J. Biol. Chem.* **277**, 5596–5602